

Quantum behaviour of a flux qubit coupled to a resonator

A. N. Omelyanchouk

B. Verkin Institute for Low Temperature Physics and Engineering, 47 Lenin Ave., 61103 Kharkov, Ukraine

S. N. Shevchenko*

*B. Verkin Institute for Low Temperature Physics and Engineering, 47 Lenin Ave., 61103 Kharkov, Ukraine and
Institute of Photonic Technology, P.O. Box 100239, D-07702 Jena, Germany*

Ya. S. Greenberg

*Novosibirsk State Technical University, 20 Karl Marx Ave., 630092 Russia and
Institute of Photonic Technology, P.O. Box 100239, D-07702 Jena, Germany*

O. Astafiev

NEC Nano Electronics Research Laboratories, Tsukuba, Ibaraki, 305-8501, Japan

E. Il'ichev

Institute of Photonic Technology, P.O. Box 100239, D-07702 Jena, Germany

(Dated: August 30, 2021)

We present a detailed theoretical analysis for a system of a superconducting flux qubit coupled to a transmission line resonator. The master equation, accounting incoherent processes for a weakly populated resonator, is analytically solved. An electromagnetic wave transmission coefficient through the system, which provides a tool for probing dressed states of the qubit, is derived. We also consider a general case for the resonator with more than one photon population and compare the results with an experiment on the qubit-resonator system in the intermediate coupling regime, when the coupling energy is comparable with the qubit relaxation rate.

Keywords: superconducting qubit, transmission line, resonator.

I. INTRODUCTION

Modern state of the art fabrication using nanotechnology brings together quantum optics and mesoscopic solid state physics. Different types of Josephson-junction quantum bits (qubits) – macroscopic quantum objects – are now intensively studied and their quantum behavior have been experimentally demonstrated (for review see e.g. [1–4]). A series of quantum phenomena such as, for example, entanglement [5, 6], Rabi oscillations [7–12], spin-echo and Ramsey fringes [13, 14], Landau-Zener-Stückelberg interferometry [15–19], have been recently demonstrated. Now, great interest is attracted to physics of artificial atoms (built on the basis of qubits) in a confined fields of electromagnetic resonators, which is known as circuit quantum electrodynamics (CQED) [20]. In pioneering CQED experiments, the artificial atom was electrostatically coupled to a high-quality transmission line resonator. The large electrical dipole moment of the qubit and high energy density of the resonator allow this system to reach the strong coupling limit. This regime was studied theoretically [21–25] and experimentally for the charge qubit coupled capacitively to the resonator [26–28]. Later inductive coupling for the flux qubit was proposed [29] and realized experimentally [30, 31].

In this paper, we analyze the system of the superconducting flux qubit coupled to the transmission line resonator. Our aim is first to present the detailed theory of the qubit's states, dressed by the interaction with the quantum resonator, and their influence on the observable transmission. Second, we describe the regime of intermediate coupling studied recently experimentally by Oelsner et al. [31]. Accordingly, the paper is organized as follows. In the next Section the model of the system is described. In Sec. III, we calculate energy levels of the system. Allowed transitions between the levels can be measured by spectroscopy applying external driving fields. Different representations of the system Hamiltonian are discussed in Sec. IV, particularly, the rotating-wave approximation (RWA), convenient for finding the stationary solutions. The analytical solution for the master equation is presented in Sec. V for the case of a weak and numeric calculations for strong driving regimes. In Appendix we present details of the theory for the transmission through the resonator.

*Electronic address: sshevchenko@ilt.kharkov.ua

II. DESCRIPTION OF THE SYSTEM

We consider the flux qubit coupled inductively to a coplanar waveguide resonator, see Fig. 1. The flux qubit is a superconducting loop with three Josephson junctions [32]. Two qubit states are naturally described in a flux basis. The two flux states ($|\uparrow\rangle, |\downarrow\rangle$) are differed by directions of the circulating current (clockwise and counterclockwise) in the loop. The qubit current interacts with the field of the resonator. The coplanar waveguide resonator is defined by two gaps in the transmission line, which form capacitances C_0 at $x = \pm l/2$. The qubit is situated close to the center of the resonator ($x = 0$), where the current of the resonator fundamental mode is maximal. Note that the qubit dimensions are significantly smaller than the resonator wavelength, therefore we consider it as a point-like object.

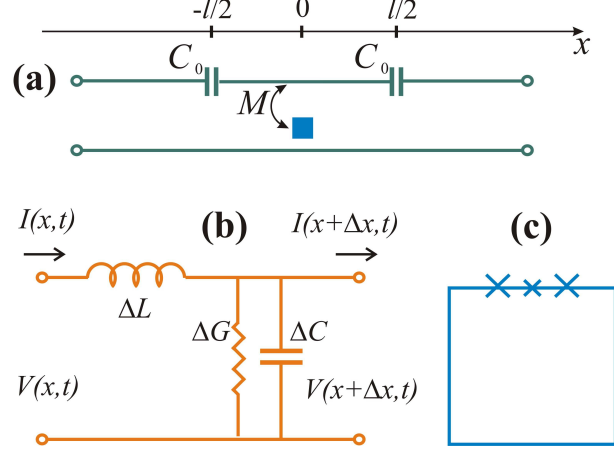


FIG. 1: (a) Schematics of the qubit (denoted by a blue box) coupled to the transmission line resonator via inductance M . (b) Equivalent circuit for the description of the infinitesimal piece of length Δx of the transmission line. (c) Flux qubit with 3 Josephson junctions.

The total Hamiltonian of the driven system

$$H = H_{\text{qb-r}} + H_{\mu\text{w}} \quad (1)$$

is a sum of the driving field Hamiltonian $H_{\mu\text{w}}$ and the qubit-resonator Hamiltonian

$$H_{\text{qb-r}} = H_{\text{qb}} + H_{\text{r}} + H_{\text{int}}, \quad (2)$$

which consists of the bare qubit H_{qb} , resonator H_{r} and the interaction term H_{int} . The flux qubit Hamiltonian in the flux basis has the form [32]

$$H_{\text{qb}} = -\frac{\Delta}{2}\sigma_x - \frac{\varepsilon}{2}\sigma_z, \quad (3)$$

where Δ is the tunnelling amplitude, the energy bias $\varepsilon = 2I_{\text{p}}(\Phi - \Phi_0/2)$ is defined by the magnetic flux Φ , I_{p} is the persistent current, $\sigma_{x,z}$ are the Pauli matrices ($\sigma_z|\downarrow\rangle = -|\downarrow\rangle$); the current operator is $\hat{I}_{\text{qb}} = -I_{\text{p}}\sigma_z$.

The qubit is coupled to the transmission line resonator. A detailed resonator description is presented in Appendix (see also Refs. [31, 33, 34]). The single-mode resonator is described by the following Hamiltonian

$$H_{\text{r}} = \hbar\omega_{\text{r}} \left(a^\dagger a + \frac{1}{2} \right), \quad (4)$$

where a and a^\dagger are the annihilation and creation operators, which act at the number (Fock) states according to $a|n\rangle = \sqrt{n}|n-1\rangle$ and $a^\dagger|n-1\rangle = \sqrt{n}|n\rangle$.

The term, describing the interaction between the resonator and the flux qubit, is

$$H_{\text{int}} = M\hat{I}(0)\hat{I}_{\text{qb}} = -\hbar g(a^\dagger + a)\sigma_z, \quad (5)$$

$$\hbar g = MI_{r0}I_p, \quad (6)$$

where M is the mutual loop-resonator inductance, $\hat{I}(0) = I_{r0}(a + a^\dagger)$ is the transmission line current operator (Eq. (A24)), at the qubit's position, $x = 0$.

The transmission line resonator is driven by the external probing voltage field at the frequency ω_d close to the resonator characteristic frequency ω_r , as described in the Appendix. The qubit in turn is driven by the resonator photon field with the amplitude ξ and the frequency ω_d . The Hamiltonian of this field, described by photon exchange between the resonator and the driving field, can be written as

$$H_{\mu w} = \xi (iae^{i\omega_d t} - ia^\dagger e^{-i\omega_d t}) \quad (7)$$

(the derivation is presented in Sec. IV)

III. ENERGY LEVELS AND THE SPECTROSCOPY OF DRESSED STATES

The qubit-resonator Hamiltonian in the qubit eigenbasis (see, e.g., Ref. [36]) can be written as

$$H'_{\text{qb-r}} = H'_0 + H'_{\text{int}}, \quad (8)$$

where

$$H'_0 = \frac{\hbar\omega_{\text{qb}}}{2}\sigma_z + \hbar\omega_r \left(a^\dagger a + \frac{1}{2} \right), \quad (9)$$

$$H'_{\text{int}} = -\hbar g (a^\dagger + a) \left(\frac{\varepsilon}{\hbar\omega_{\text{qb}}}\sigma_z - \frac{\Delta}{\hbar\omega_{\text{qb}}}\sigma_x \right), \quad (10)$$

with the bare qubit energy splitting

$$\hbar\omega_{\text{qb}} = \sqrt{\Delta^2 + \varepsilon^2}. \quad (11)$$

The bare system eigenstates are $|e/g, n\rangle = |e/g\rangle \otimes |n\rangle$ and eigenvalues

$$E_{e/g, n} = \pm \frac{\hbar\omega_{\text{qb}}}{2} + \hbar\omega_r \left(n + \frac{1}{2} \right). \quad (12)$$

The states $|e, n\rangle$ and $|g, n+1\rangle$ are degenerated at $\omega_r = \omega_{\text{qb}}$ and the degeneracy is lifted by the qubit-resonator interaction. The transition matrix element due to the interaction is

$$\langle g, n+1 | H'_{\text{int}} | e, n \rangle = \langle e, n | H'_{\text{int}} | g, n+1 \rangle = \hbar g_\varepsilon \sqrt{n+1}, \quad (13)$$

where the qubit-resonator interaction energy is

$$\hbar g_\varepsilon = \hbar g \frac{\Delta}{\hbar\omega_{\text{qb}}}. \quad (14)$$

Note that the coupling strength is scaled as $\Delta/\hbar\omega_{\text{qb}}$ [21]. The eigenvectors $|+\rangle$ and $|-\rangle$ of the total Hamiltonian $H'_{\text{qb-r}}$ are obtained from the non-interacting qubit-resonator basis by the following transformation

$$\begin{pmatrix} |-, n\rangle \\ |+, n\rangle \end{pmatrix} = \begin{pmatrix} \sin \eta & \cos \eta \\ -\cos \eta & \sin \eta \end{pmatrix} \begin{pmatrix} |g, n+1\rangle \\ |e, n\rangle \end{pmatrix}, \quad (15)$$

where

$$\tan 2\eta = \frac{2g_\varepsilon \sqrt{n+1}}{\delta}, \quad (16)$$

$$E_{\pm, n} = \hbar\omega_r (n+1) \pm \frac{\hbar\Omega_n}{2}, \quad (17)$$

$$\Omega_n = \sqrt{4g_\varepsilon^2(n+1) + \delta^2}, \quad (18)$$

$$\delta = \omega_{\text{qb}} - \omega_r < 0. \quad (19)$$

The energy of the ground state, $|g, 0\rangle$, is given by

$$E_{\text{gr}} \equiv E_{g,0} = -\frac{\hbar\delta}{2}. \quad (20)$$

Here Ω_n defines the energy difference $E_{+,n} - E_{-,n} = \hbar\Omega_n$. In particular, the energy anticrossing takes place at $\delta = 0$, that is at $\hbar\omega_{\text{qb}}(\varepsilon^*) = \hbar\omega_r$, and it is given by

$$\Omega_n^{\text{min}} = \Omega_n(\varepsilon^*) = 2g_{\varepsilon^*}\sqrt{n+1} = 2g\frac{\Delta}{\hbar\omega_r}\sqrt{n+1}. \quad (21)$$

For example, in the inset of Fig. 2(a), the energy anticrossing is shown for $n = 0$.

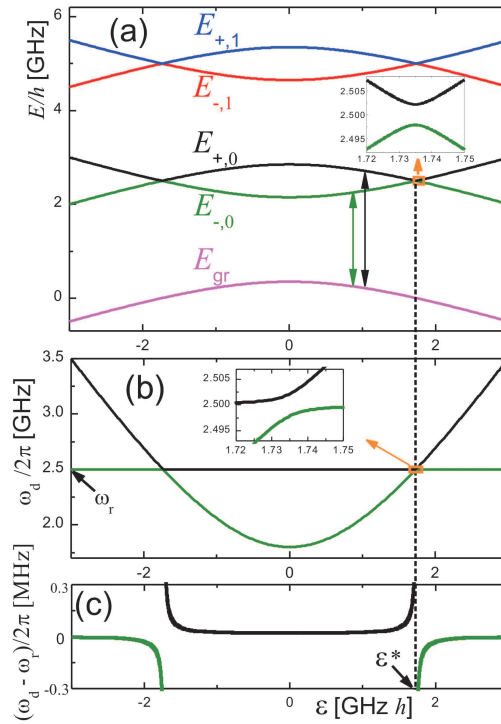


FIG. 2: Energy diagrams calculated for the following qubit parameters $\Delta/h = 1.8$ GHz, $g/2\pi = 3$ MHz, $\omega_r/2\pi = 2.5$ GHz. (a) Energy levels versus energy bias ε . Avoided level crossing is shown as a close-up in the inset. (b) Contour lines of the energy difference versus bias ε and the driving frequency ω_d . The green (lower) line is for $\hbar\omega_d = E_{-,0} - E_{\text{gr}}$ and the black (upper) line is for $\hbar\omega_d = E_{+,0} - E_{\text{gr}}$. (c) The same plot as in (b) but in a narrow vicinity to the resonator fundamental frequency ω_r .

If the resonator is driven by a weak external field, so that it is weakly populated, one can limit the consideration by a few Fock states, neglecting unpopulated levels; the energy levels are plotted with Eqs. (17) and (20) in Fig. 2(a). With the weak driving field the spectroscopy of the "dressed" energy levels can be done: the transmission is resonantly increased when the driving photon energy $\hbar\omega_d$ matches the system energy difference of Eqs. (17) and (20), shown by two arrowed lines in Fig. 2(a) for two possible transitions. One can plot then the respective energy contour lines to describe experimental results (see Figs. 2(b, c)), which relates to the experimental data presented in Figs. 2 and 3 of Ref. [31]. With increasing driving amplitude, higher order processes such as multi-photon transitions may become possible [30, 37].

IV. HAMILTONIAN OF THE SYSTEM

Jaynes-Cummings Hamiltonian. Let us rewrite the interaction Hamiltonian, Eq. (10), by introducing the qubit lowering and raising operators

$$\sigma^\pm = \frac{1}{2}(\sigma_x \pm i\sigma_y), \quad (22)$$

so that $\sigma^+ |g\rangle = |e\rangle$, $\sigma^+ |e\rangle = 0$, etc.; then we have

$$H'_{\text{int}} = \hbar g_\varepsilon (a^\dagger \sigma^- + a \sigma^+) + \hbar g_\varepsilon (a \sigma^- + a^\dagger \sigma^+) - \hbar g \frac{\varepsilon}{\hbar \omega_{\text{qb}}} (a^\dagger + a) \sigma_z. \quad (23)$$

In vicinity of degeneracy of the states $|e, n\rangle$ and $|g, n+1\rangle$, the second and the third term in Eq. (23) can be neglected as they correspond to the processes, which require large extra energy. The first term together with H'_0 from Eq. (9) give the Jaynes-Cummings Hamiltonian

$$H_{\text{JC}} = \frac{\hbar \omega_{\text{qb}}}{2} \sigma_z + \hbar \omega_r \left(a^\dagger a + \frac{1}{2} \right) + \hbar g_\varepsilon (a^\dagger \sigma^- + a \sigma^+). \quad (24)$$

Interaction representation. We consider H'_{int} in the interaction representation. For this, we note the following relations (see e.g. [38])

$$e^{ia^\dagger a \omega t} a e^{-ia^\dagger a \omega t} = a e^{-i\omega t}, \quad (25)$$

$$e^{i\frac{\omega}{2} t \sigma_z} \sigma^- e^{-i\frac{\omega}{2} t \sigma_z} = \sigma^- e^{-i\omega t}. \quad (26)$$

Then we obtain

$$\begin{aligned} H_{\text{int}}^I &= e^{\frac{i}{\hbar} H'_0 t} H'_{\text{int}} e^{-\frac{i}{\hbar} H'_0 t} = \hbar g_\varepsilon \left(a \sigma^+ e^{i(\omega_{\text{qb}} - \omega_r) t} + h.c. \right) \\ &+ \hbar g_\varepsilon \left(a \sigma^- e^{-i(\omega_{\text{qb}} + \omega_r) t} + h.c. \right) - \hbar g \frac{\varepsilon}{\hbar \omega_{\text{qb}}} \left(a e^{-i\omega_r t} + h.c. \right). \end{aligned} \quad (27)$$

In the RWA, when $\omega_{\text{qb}} - \omega_r \ll \omega_{\text{qb}}$, the first term is slowly rotating, while the second and third terms are fast rotating ones. This justifies neglecting these terms.

Driving Hamiltonian. We will consider scattering of the right propagating wave $V_1^r(e^{-ik(x+l/2)+i\omega_d t} + c.c.)$ on the resonator (see Eq. (A31)), where V_1^r is chosen to be a real amplitude. This wave drives the resonator, which in turn generates the scattered waves. Using semiclassical approach, we first consider the driving dynamics under the classical field and then calculate the field generated by the resonator. The calculated first order scattering gives an exact solution because the two scattered waves, propagating in different directions cancel out the second order driving effect (see Eq. (A64)). The dipole-like interaction Hamiltonian can be presented as a product of the incident wave voltage field and charges generated by the resonator field on the coupling capacitances $C_0 V_{r0}(ia - ia^\dagger) \sin(\pm k_r l/2)$ (see Eq. (A27))

$$H_{\mu w} = \xi \left(e^{i\omega_d t} + e^{-i\omega_d t} \right) (ia - ia^\dagger), \quad (28)$$

where

$$\xi = C_0 V_1^r V_{r0} \sin(k_r l/2) (-1 + e^{-ik_r l}) = -2C_0 V_1^r V_{r0}. \quad (29)$$

And omitting fast rotating terms in RWA, we arrive to Eq. (7). In these equations we assume $\theta_1 = \omega C_0 Z_1 \ll 1$, which is valid for high quality resonators.

Rotating-wave approximation. We consider the Hamiltonian of the *driven* system in the RWA

$$H_{\text{RWA}} = U \left(H'_{\text{qb-r}} + H_{\mu w} \right) U^\dagger + i\hbar \dot{U} U^\dagger. \quad (30)$$

For this we choose the transformation

$$U = \exp \left[i\omega_d t \left(a^\dagger a + \sigma_z/2 \right) \right] \quad (31)$$

and obtain

$$H_{\text{RWA}} = \hbar \frac{\delta\omega_{\text{qb}}}{2} \sigma_z + \hbar \delta\omega_{\text{r}} a^\dagger a + \hbar g_\varepsilon (a\sigma^+ + a^\dagger\sigma^-) + \xi(ia - ia^\dagger), \quad (32)$$

$$\begin{aligned} \delta\omega_{\text{qb}} &= \omega_{\text{qb}} - \omega_{\text{d}}, \\ \delta\omega_{\text{r}} &= \omega_{\text{r}} - \omega_{\text{d}}. \end{aligned} \quad (33)$$

Control microwave field. For the sake of generality, we consider also the case when the qubit is driven by the separate microwave field, coupled, for example via an additional microwave line. Then, we have

$$H_{\mu\text{w}}^{(2)} = -I_{\text{p}} \Phi_{\text{ac}} \cos \omega_{\text{d}} t \cdot \sigma_z, \quad (34)$$

where Φ_{ac} is the amplitude of the driving flux. In the qubit eigenstate representation, this is simplified to the form of Eq. (7) according to

$$H_{\mu\text{w}}^{(2)'} = -I_{\text{p}} \Phi_{\text{ac}} \frac{e^{i\omega_{\text{d}} t} + e^{-i\omega_{\text{d}} t}}{2} \left(\frac{\varepsilon}{\hbar\omega_{\text{qb}}} \sigma_z - \frac{\Delta}{\hbar\omega_{\text{qb}}} \sigma_x \right) \approx \xi_\varepsilon (e^{i\omega_{\text{d}} t} \sigma^- + e^{-i\omega_{\text{d}} t} \sigma^+), \quad (35)$$

$$\xi_\varepsilon = \frac{1}{2} I_{\text{p}} \Phi_{\text{ac}} \frac{\Delta}{\hbar\omega_{\text{qb}}}. \quad (36)$$

Here we have left only slowly rotating terms (see discussion above). Note that the amplitude ξ_ε is dependent on the bias ε (see Eq. (11)). Then in the RWA after the transformation (31) we obtain the expression which differs from Eq. (32) by substituting the last term with $\xi_\varepsilon(\sigma^+ + \sigma^-)$.

Dispersive regime. In the dispersive regime (when $\delta \gg \hbar g_\varepsilon$) the diagonalization of the Hamiltonian (24) in the second order in g/δ [38] gives

$$H = -\frac{1}{2} \left(\hbar\omega_{\text{qb}} + \frac{\hbar g_\varepsilon^2}{\delta} \right) \sigma_z + \left(\hbar\omega_{\text{r}} + \frac{\hbar g_\varepsilon^2}{\delta} \sigma_z \right) a^\dagger a. \quad (37)$$

This expression explicitly shows the qubit transition energy shift by the coupling and also the resonator energy shift by the qubit, which sign depends on the qubit state.

V. SOLUTION OF THE MASTER EQUATION FOR THE DENSITY MATRIX OF THE SYSTEM

To describe the qubit-resonator dissipative and incoherent dynamics we assume that all processes in our system are Markovian and solve the master equation for the density matrix ρ

$$\dot{\rho} = -\frac{i}{\hbar} [H, \rho] + \mathcal{L}[\rho]. \quad (38)$$

It includes the dynamic part and dissipative Lindblad term [39]

$$\mathcal{L}[\rho] = \frac{1}{2} \sum_{k=1}^3 \left(2C_k \rho C_k^\dagger - C_k^\dagger C_k \rho - \rho C_k^\dagger C_k \right), \quad (39)$$

where

$$\begin{aligned} C_1 &= \sqrt{\gamma_1} \sigma, \quad \gamma_1 = \frac{1}{T_1}, \\ C_2 &= \sqrt{\frac{\gamma_\phi}{2}} \sigma_z, \quad \gamma_\phi = \frac{1}{T_\phi} = \frac{1}{T_2} - \frac{1}{2T_1}, \\ C_3 &= \sqrt{\varkappa} a. \end{aligned} \quad (40)$$

The Lindblad operator \mathcal{L} presents dissipation in the resonator (photon decay) with the rate $\varkappa = \varkappa_{\text{ext}} + \varkappa_{\text{int}}$, where \varkappa_{ext} and \varkappa_{int} are external (leaking out through of the resonator) and internal (resistive) loss rates, and the qubit decoherence consisting of the relaxation rate γ_1 and the dephasing rate γ_ϕ . Here we consider nondispersive regime (near the qubit-resonator resonance). The Hamiltonian of the system H in the rotating wave approximation has the form of Eq. (32). The solution of the master equation determines the observable quantities, in particular, the expectation value of the photon field in the resonator

$$\langle a \rangle = \text{Tr}(a\rho). \quad (41)$$

The Hilbert space of the composite system is the tensor product of the qubit space and the photon space with basis vectors $|e/g, n\rangle = |e/g\rangle \otimes |n\rangle$. Basis vectors $|g\rangle$ and $|e\rangle$

$$|g\rangle = \begin{bmatrix} 0 \\ 1 \end{bmatrix}, \quad |e\rangle = \begin{bmatrix} 1 \\ 0 \end{bmatrix} \quad (42)$$

are the eigenvectors of the operator σ_z . Vectors of Fock (photon) states $|n\rangle$ (the eigenvectors of the photon number operator $a^\dagger a$ $|n\rangle = n|n\rangle$) are the vectors in the infinite-dimensional space $N = \infty$

$$|0\rangle = \begin{bmatrix} 1 \\ 0 \\ 0 \\ \vdots \end{bmatrix}, |1\rangle = \begin{bmatrix} 0 \\ 1 \\ 0 \\ \vdots \end{bmatrix}, |2\rangle = \begin{bmatrix} 0 \\ 0 \\ 1 \\ 0 \\ \vdots \end{bmatrix}, \dots |n\rangle = \begin{bmatrix} 0 \\ 0 \\ \vdots \\ 1 \\ \vdots \end{bmatrix}. \quad (43)$$

In the basis $|e/g, n\rangle$ the matrix equation (38) is the infinite set of equations for the infinite-dimensional matrix ρ_{ij} .

Below, we consider the simplest case of $N = 2$ (weak driving limit), where the analytical solution is possible, and in the case of $N \gg 1$ we study the problem numerically.

A. Weak driving limit

To find the analytical solution we restrict the photon space to $N = 2$, assuming that the mean photon number in the resonator (created by the driving field with the amplitude ξ) is much less than unity. The basis $|e/g, n\rangle$ in this case consists of 4 base vectors b_i

$$b_1 = |g0\rangle, b_2 = |e0\rangle, b_3 = |g1\rangle, b_4 = |e1\rangle, \quad (44)$$

and the density matrix $\rho_{ij} = \langle b_i | \rho | b_j \rangle$ takes the form

$$\rho = \begin{pmatrix} \rho_{e0,e0} & \rho_{e0,g0} & \rho_{e0,e1} & \rho_{e0,g1} \\ \rho_{g0,e0} & \rho_{g0,g0} & \rho_{g0,e1} & \rho_{g0,e1} \\ \rho_{e1,e0} & \rho_{e1,e0} & \rho_{e1,e1} & \rho_{e1,g1} \\ \rho_{g1,e0} & \rho_{g1,g0} & \rho_{g1,e1} & \rho_{g1,g1} \end{pmatrix}. \quad (45)$$

In the steady state from Eq. (38) we have 16 linear equations for the matrix elements ρ_{ij} . In the weak driving limit, when the drive does not change population of the ground state $\rho_{g0,g0} = 1$, leaving up to the first order terms only in the amplitude ξ , we obtain the density matrix ρ . The nonzero elements of the matrix ρ_{ij} are

$$\begin{aligned} \rho_{g0,g0} &= 1, \\ \rho_{g1,g0} &= \rho_{g0,g1}^* = \frac{-i(\xi/\hbar)(\delta\omega_{\text{qb}} - i\gamma)}{g_\varepsilon^2 - (\delta\omega_{\text{r}} - i\frac{\varkappa}{2})(\delta\omega_{\text{qb}} - i\gamma)}, \\ \rho_{e0,g0} &= \rho_{g0,e0}^* = \frac{-i(\xi/\hbar)g_\varepsilon}{g_\varepsilon^2 - (\delta\omega_{\text{r}} - i\frac{\varkappa}{2})(\delta\omega_{\text{qb}} - i\gamma)}, \end{aligned} \quad (46)$$

where $\gamma = \frac{\gamma_1}{2} + \gamma_\phi$.

Using (45) in (41) we obtain for the mean value of the voltage field in the resonator in the weak driving (WD) limit for positive frequencies

$$V_{r0} \langle -ia^\dagger \rangle_{\text{WD}} = V_{r0} \frac{\xi(\delta\omega_{qb} + i\gamma)}{g_\varepsilon^2 - (\delta\omega_r + i\frac{\kappa}{2})(\delta\omega_{qb} + i\gamma)}. \quad (47)$$

The transmission coefficient of the output driving signal t is defined by the photon field in the resonator, Eq. (A63), and according with (47) we obtain

$$t_{\text{WD}} = -i \frac{\kappa_{\text{ext}}}{2} \frac{\delta\omega_{qb} + i\gamma}{g_\varepsilon^2 - (\delta\omega_r + i\frac{\kappa}{2})(\delta\omega_{qb} + i\gamma)}. \quad (48)$$

When $g_\varepsilon = 0$, this equation gives the transmission coefficient through the resonator, which for the linear resonator can be derived classically (Eq. A40). The plot of the transmission amplitude $|t|_{\text{WD}}$, given by Eq. (48), is shown in Fig. 3 for $\omega_{qb} = \omega_r$ and different values of the decay rates κ and γ (given in units of the coupling constant g_ε). For weak decay rates κ and γ , the transmission spectrum displays the Rabi-splitting peaks (red solid curve), which are smeared with increasing of the decay.

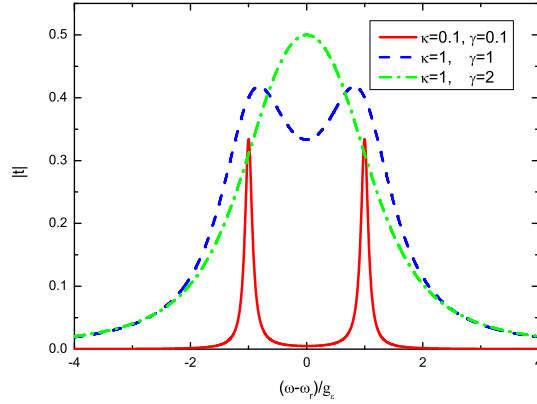


FIG. 3: Normalized transmission amplitude $|t|$ as a function of the driving frequency detuning $\omega_d - \omega_r$ at $\varepsilon = \varepsilon^*$ (when $\omega_{qb}(\varepsilon^*) = \omega_r$) for different values of the decay rates κ and γ (given in the figure in units of g_ε), calculated with Eq. (48).

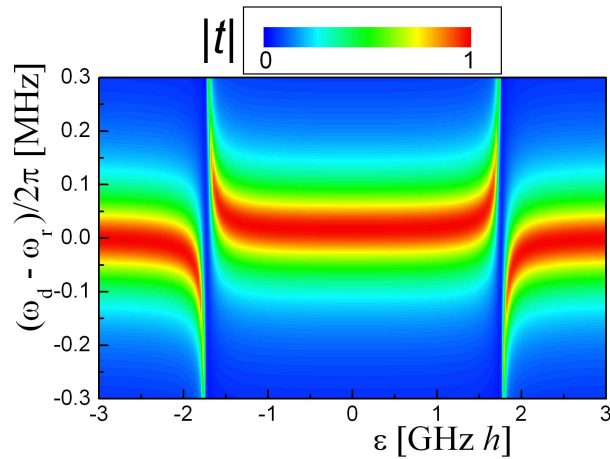


FIG. 4: Normalized transmission amplitude $|t|$ as a function of the bias ε and the driving frequency detuning $\omega_d - \omega_r$, calculated with Eq. (48).

In Fig. 4 the density plot of the transmission amplitude as a function of the bias ε and the detuning $\omega_d - \omega_r$ is shown. The parameters here and below are taken for the comparison with the relevant experimental work [31] $\Delta/h = 1.8$ GHz, $g/2\pi = 3$

MHz, $\omega_r/2\pi = 2.5$ GHz (the same as in Fig. 2) and also the loss rate of the resonator $\kappa/2\pi = 1.25 \cdot 10^{-4}$ GHz and the loss rate of the qubit $\gamma = g$. Note that we consider the intermediate coupling regime, when $g = \gamma \gg \kappa$. The transmission amplitude is resonantly increased along the lines shown in Fig. 2(c) as expected. In the narrow vicinity of the resonator characteristic frequency, $\omega_d \in (\omega_r - g, \omega_r + g)$, the avoided crossing at $\varepsilon = \varepsilon^*$ is demonstrated, as it was reported in Ref. [31].

For more detailed comparison and finding the parameters with better accuracy (e.g. decay rate γ), we need to compare experimental and theoretical sets of cross-section of surfaces $|t|$ versus ε and ω_d . This is shown in Fig. 5 for $\omega_d = \omega_r$.

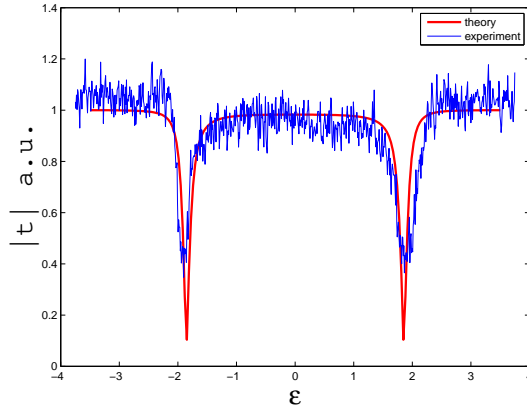


FIG. 5: Normalized transmission amplitude $|t|$ as a function of the bias ε for $\omega_d = \omega_r$ calculated with Eq. (48), red line, and obtained experimentally, blue line.

B. Numerical solution of the master equation. Beyond the weak driving regime.

In the case, when driving is not weak, i.e. the mean photon number $\langle a^\dagger a \rangle \gtrsim 1$, we have solved the equation for the density matrix ρ numerically. The results are presented in Fig. 6. The transmission amplitude $|t|$ in all cases is normalized on the maximal value at $\omega_{qb} = \omega_r$. In Fig. 6(a) the transmission amplitude is shown for the case of small damping $\kappa/g_\varepsilon = 0.1$ and $\gamma/g_\varepsilon = 0.1$. At a weak driving amplitude ξ the red curve in Fig. 6(a) coincides with $|t|_{\text{WD}}(\omega_d)$ (Fig. 3). With increasing ξ , each split Rabi peak is additionally split (blue curve) (see also in Ref. [40]). With further increasing of the amplitude ξ , the additional splitting is smeared (green curve). Thus in the nonlinear regime we observe the qualitatively new features as compared to the weak driving limit. When the decay is rather large, such that in the weak-driving case, we do not have the Rabi splitting (green curve in Fig. 3), in the nonlinear response, we do not observe the qualitatively new features, as shown in Fig. 6(b) ($\kappa/g_\varepsilon = 1$ and $\gamma/g_\varepsilon = 2$).

We also calculate the average number of photons in the resonator, $n = \langle a^\dagger a \rangle$. For the parameters in Fig. 6, it depends on the frequency; the maximal values are the following $n_{\text{max}} = 0.005$ for $\xi/g_\varepsilon = 0.01$, $n_{\text{max}} = 0.3$ for $\xi/g_\varepsilon = 0.15$, $n_{\text{max}} = 1.8$ for $\xi/g_\varepsilon = 0.3$.

VI. CONCLUSION

We presented the detailed theory for the system of the flux qubit coupled inductively to the transmission line resonator. The transmission coefficient is calculated with the system's density matrix by solving the master equation within RWA.

The avoided crossing of the dressed energy levels is shown in the resonant case, where $\omega_d \approx \omega_{qb} \approx \omega_r$. This is demonstrated in the intermediate coupling regime, which describe the experimental results of Oelsner et al. [31]. We have shown that the dissipation smears the Rabi splitting. Moreover, we have demonstrated the double splitting in the strong driving regime.

Acknowledgments

This work was supported by the Fundamental Researches State Fund grant F28.2/019, by the EU through the EuroSQIP project, by the DFG project IL 150/6-1, by DAAD scholarship A/10/05536. Ya. S. G. and E. I. acknowledge the financial support from Federal Agency on Science and Innovations of Russian Federation under contract No. 02.740.11.5067 and the

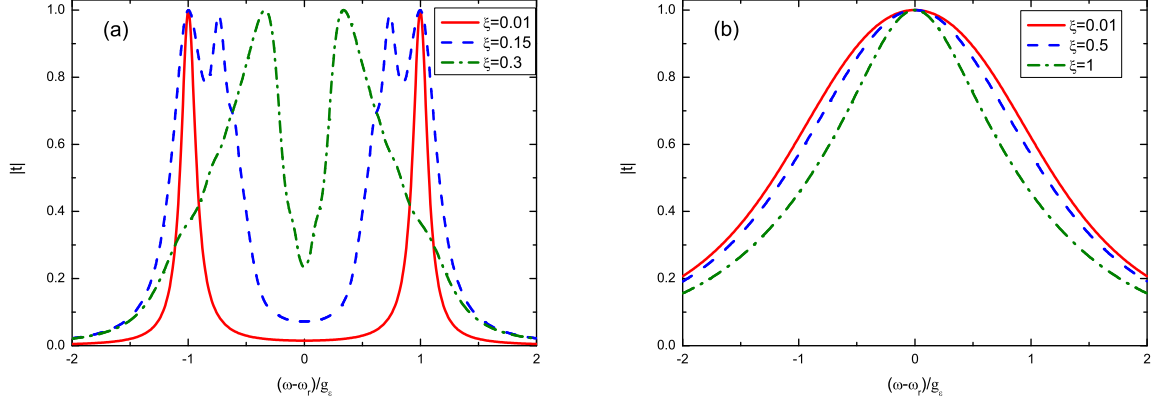


FIG. 6: Normalized transmission amplitude $|t|$ as a function of the driving frequency detuning $\omega_d - \omega_r$ at $\varepsilon = \varepsilon^*$ (when $\omega_{qb}(\varepsilon^*) = \omega_r$) for (a) $\varkappa/g_\varepsilon = 0.1$, $\gamma/g_\varepsilon = 0.1$ and (b) $\varkappa/g_\varepsilon = 1$, $\gamma/g_\varepsilon = 2$, calculated by solving numerically the master equation for several values of ξ , given in units of g_ε .

financial support from Russian Foundation for Basic Research, Grant RFBR-FRSFU No. 09-02-90419. Ya. S. G. and S. N. Sh. thank P. Macha and G. Oelsner for valuable discussions.

Appendix A: Transmission line resonator

In this Appendix we consider the resonator formed by the transmission line interrupted by two capacitances C_0 . The qubit we assume to be coupled inductively to the resonator at its center, see Fig. 1(a). We start by presenting the equations which describe the transmission line.

1. The transmission line

The transmission line is usually modelled as an infinite series of the elementary circuits (e.g., [41]), as shown in Fig. 1(b). Here elementary inductance, capacitance and conductance are $\Delta L = L\Delta x$, $\Delta C = C\Delta x$, $\Delta G = G\Delta x$, where L , C and G are inductance, capacitance and conductance (of parallel resistance) per unit length. For the circuit in Fig. 1(b), we can write (neglecting the Ohmic losses) the equations for the transmission line, by applying the Kirchhoff's laws for the voltage $V(x, t)$ and the current $I(x, t)$; in the limit $\Delta x \rightarrow 0$ they take the form

$$\frac{\partial V(x, t)}{\partial x} = -L \frac{\partial I(x, t)}{\partial t}, \quad (\text{A1})$$

$$\frac{\partial I(x, t)}{\partial x} = -GV(x, t) - C \frac{\partial V(x, t)}{\partial t}. \quad (\text{A2})$$

These equations can be rewritten for either $I(x, t)$ or $V(x, t)$ as following

$$\frac{\partial^2 A}{\partial x^2} - \frac{1}{v^2} \frac{\partial^2 A}{\partial t^2} = \frac{\varkappa}{v^2} \frac{\partial A}{\partial t}, \quad A = \{I, V\}, \quad (\text{A3})$$

$$v = 1/\sqrt{LC}, \quad (\text{A4})$$

$$\varkappa = G/C. \quad (\text{A5})$$

Here v is the phase velocity and \varkappa defines the loss in the transmission line.

Assuming $I(x, t) = I(x)e^{i\omega t}$ and $V(x, t) = V(x)e^{i\omega t}$, we obtain

$$\frac{dV(x)}{dx} = -i\omega LI(x), \quad (\text{A6})$$

$$\frac{dI(x)}{dx} = -(G + i\omega C)V(x). \quad (\text{A7})$$

Then equation for $A(x) = \{I(x), V(x)\}$ can be written as following

$$\frac{d^2 A(x)}{dx^2} - \gamma^2 A(x) = 0, \quad (\text{A8})$$

$$\gamma = \sqrt{i\omega L(G + i\omega C)} \equiv \alpha + ik. \quad (\text{A9})$$

Solving equation for $V(x)$ and using Eq. (A6), we obtain

$$V(x) = V_0^r e^{-\gamma x} + V_0^l e^{\gamma x}, \quad (\text{A10})$$

$$I(x) = \frac{V_0^r}{Z_0} e^{-\gamma x} - \frac{V_0^l}{Z_0} e^{\gamma x}, \quad (\text{A11})$$

where

$$Z_0 = \frac{i\omega L}{\gamma} \equiv Z_1 + iZ_2. \quad (\text{A12})$$

$$Z_1 = \frac{\omega Lk}{\alpha^2 + k^2}, \quad Z_2 = \frac{\omega L\alpha}{\alpha^2 + k^2}. \quad (\text{A13})$$

When losses in the line are small ($G \ll \omega C$), we obtain

$$k \approx \omega\sqrt{LC} = \frac{\omega}{v}, \quad \alpha \approx \frac{G}{2} \sqrt{\frac{L}{C}} = \frac{\varkappa}{2v}, \quad (\text{A14})$$

$$Z_1 = \sqrt{\frac{L}{C}}, \quad Z_2 = \frac{\omega L\alpha}{k^2}. \quad (\text{A15})$$

Here the constants V_0^r and V_0^l are the amplitudes of the right- and left-moving waves and Z_0 is the transmission line characteristic (wave) impedance.

2. Open transmission-line resonator

We consider the open transmission line of the length l . The quality factor of the resonator [41] can be written as

$$Q = \frac{k}{2\alpha} = \frac{\omega_r C}{G} = \frac{\omega_r}{\varkappa}. \quad (\text{A16})$$

Now let us define normal modes of the resonator without dissipation ($\varkappa = 0$). Then assuming zero current through the boundaries at $x = \pm l/2$ for this modes, we obtain

$$I^{(j)}(x) = \frac{V_0^r}{Z_0} (e^{-ik_j x} - (-1)^j e^{ik_j x}), \quad (\text{A17})$$

$$V^{(j)}(x) = V_0^r (e^{-ik_j x} + (-1)^j e^{ik_j x}), \quad (\text{A18})$$

where $k_j l = j\pi$, $j = 1, 2, 3, \dots$. In particular, for the fundamental mode $j = 1$ of the resonator we obtain

$$I^{(1)}(x) = \frac{2V_0^r}{Z_0} \cos k_1 x, \quad (\text{A19})$$

$$V^{(1)}(x) = -2iV_0^r \sin k_1 x. \quad (\text{A20})$$

For the fundamental mode $j = 1$ of the $\lambda/2$ resonator ($l = \lambda/2$), we have $k_r \equiv k_1 = \pi/l$, $\omega_r \equiv \omega_1 = k_1 v = \frac{2\pi}{2\sqrt{L_r C_r}}$, where $L_r = Ll$ and $C_r = Cl$ are the total inductance and capacitance of the resonator.

Quantization of the resonator eigenmodes results in the following expressions for the current and voltage operators and the Hamiltonian

$$\hat{I} = \sum \sqrt{\frac{\hbar\omega_j}{L_r}} (a_j + a_j^\dagger) \cos k_j x, \quad (\text{A21})$$

$$\hat{V} = -i \sum \sqrt{\frac{\hbar\omega_j}{C_r}} (a_j - a_j^\dagger) \sin k_j x, \quad (\text{A22})$$

$$\hat{H}_r = \sum \hbar\omega_j \left(a_j^\dagger a_j + \frac{1}{2} \right). \quad (\text{A23})$$

We consider the frequency close to the fundamental mode frequency ω_r , and, therefore, we ignore other modes. For the fundamental mode, with $k_1 = \pi/l$ and omitting the index $j = 1$, we obtain

$$\hat{I} = I_{r0}(a + a^\dagger) \cos \frac{\pi x}{l}, \quad I_{r0} = \sqrt{\frac{\hbar\omega_r}{L_r}}, \quad (\text{A24})$$

$$\hat{V} = iV_{r0}(a - a^\dagger) \sin \frac{\pi x}{l}, \quad V_{r0} = \sqrt{\frac{\hbar\omega_r}{C_r}}, \quad (\text{A25})$$

where I_{r0} and V_{r0} are the zero-point root mean square (rms) current and voltage, and the Hamiltonian is given by Eq. (4).

We also consider the realistic case: the resonator with two point-like coupling capacitances C_0 at the ends with $\theta_1 = \omega C_0 Z_1 \ll 1$. For the fundamental mode, the current and voltage operators are modified to

$$\hat{I} = I_{r0}(a + a^\dagger) \cos k_r x, \quad (\text{A26})$$

$$\hat{V} = V_{r0}(ia - ia^\dagger) \sin k_r x. \quad (\text{A27})$$

And we find

$$k_r \approx k_1 - \frac{2\theta_1}{l} \quad (\text{A28})$$

from the boundary conditions

$$I_{r0}(a + a^\dagger) \cos(\pm k_r l/2) = V_{r0}[ia(-i\omega C_0) - ia^\dagger i\omega C_0] \sin(\pm k_r l/2). \quad (\text{A29})$$

This results in the shifted resonant frequency

$$\omega_r = \omega_1 \left(1 - \frac{2\theta_1}{\pi} \right), \quad (\text{A30})$$

which is slightly lower than the fundamental frequency ω_1 , due to external coupling to the outside lines via the capacitance C_0 .

3. Transmission through the coplanar waveguide resonator

Now we will consider a classical problem of transmission of waves through the resonator. It will help us to find correspondence between the classical and quantum-mechanical solutions and to define the photon decay rates. The incident wave propagates from left to right and interacts with the transmission-line resonator at $x = -l/2$ through the capacitance C_0 . The output wave is detected after another capacitance C_0 at $x = l/2$. We will obtain the system of equations for V_j^r and V_j^l , which define the classical current and voltage in j -th region, $j = 1, 2, 3$, respectively for $x < -l/2$, $x \in (-l/2, l/2)$, and $x > l/2$;

$$V_j(x) = V_j^r e^{-\gamma(x-x_j)} + V_j^l e^{\gamma(x-x_j)}, \quad (\text{A31})$$

$$I_j(x) = \frac{V_j^r}{Z_0} e^{-\gamma(x-x_j)} - \frac{V_j^l}{Z_0} e^{\gamma(x-x_j)}, \quad (\text{A32})$$

where $x_1 = -l/2$, $x_2 = 0$ and $x_3 = l/2$. We assume the matched termination (with impedance equal to Z_0), then there is no left-propagating wave in the third region, $V_3^l = 0$. The boundary conditions for currents and voltages at the points $x = \pm l/2$ are the following

$$I_1(-l/2) = I_2(-l/2), \quad (\text{A33})$$

$$I_2(l/2) = I_3(l/2), \quad (\text{A34})$$

$$V_1(-l/2) = V_2(-l/2) + I_2(-l/2)/i\omega C_0, \quad (\text{A35})$$

$$V_2(l/2) = V_3(l/2) + I_3(l/2)/i\omega C_0. \quad (\text{A36})$$

From these equations, substituting $V_1(-l/2) = V_1^r + V_1^l$, we find a useful relation between the field in the resonator and the external field V_3

$$V_3(l/2) = V_2(l/2) \frac{i\theta_1}{1 + i\theta_1}, \quad (\text{A37})$$

where $\theta_1 = \omega C_0 Z_1$.

We define the transmission coefficient t as a ratio between the transmitted wave and the incident one as

$$t = \frac{V_3^r}{V_1^r} \quad (\text{A38})$$

and find directly from Eqs. (A31-A35)

$$t = \frac{4\theta_1^2 e^{-\gamma l}}{4\theta_1^2 - 4i\theta_1 - 1 + e^{-2\gamma l}}. \quad (\text{A39})$$

For the interesting case of high-Q resonators ($\alpha \ll k$ and $\theta \approx \omega C_0 Z_1 \ll 1$), we can express the transmission coefficient near the fundamental mode ($\omega_1 = v\pi/l$) in the compact form

$$t \approx \frac{\varkappa_{\text{ext}}}{1 - i \frac{2\delta\omega}{\varkappa}}, \quad (\text{A40})$$

where $\delta\omega = \omega_r - \omega_d$ is detuning from the resonant frequency

$$\omega_r = \omega_1 \left(1 - \frac{2\theta_1}{\pi} \right) \quad (\text{A41})$$

due to coupling capacitance C_0 . Note that this formula coincides with Eq. (A30), however, obtained from the classical solution. The peak width

$$\Delta\omega = \varkappa, \quad (\text{A42})$$

is determined by the total photon decay rate $\varkappa = \varkappa_{\text{ext}} + \varkappa_{\text{int}}$ which is the sum of the photon decay rate due to the external loss

$$\varkappa_{\text{ext}} = \frac{4\theta_1^2 \omega_r}{\pi} \quad (\text{A43})$$

determined by the coupling to the external transmission lines via C_0 and the internal photon decay rate

$$\varkappa_{\text{int}} = \frac{2\alpha\omega_r}{\pi} \quad (\text{A44})$$

due to dissipations within the resonator. The quality factor is

$$Q = \frac{\omega_r}{\Delta\omega} = \frac{\pi}{4\theta_1^2 + 2\alpha l}. \quad (\text{A45})$$

This rate is consistent with its definition given in Ref. [31].

Below we estimate the photon decay rate \varkappa for the coplanar waveguide resonator with parameters taken from [42] $l = 23$ mm, $\omega_r/2\pi = 2.5$ GHz, $C_0 = 1$ fF, $Z_1 = 50$ Ohm, which give $\theta_1 = 7.8 \times 10^{-4}$. The capacitance per unit length C is calculated from the expression for θ_1 at resonance $\theta_1 = \pi C_0/lC$. We thus obtain $C = 1.74 \times 10^{-10}$ F/m. Finally, for the photon decay rate \varkappa we obtain $\varkappa/2\pi = 1.95$ kHz. This value is about two times smaller than the ones obtained in [42]. We assume that this discrepancy is due to dielectric losses G . It allows us to estimate α from $4\theta_1^2 \approx 2\alpha l$, then $\alpha \approx 5.3 \times 10^{-5} \text{ m}^{-1}$. Therefore, for G we obtain $G = 2\alpha/Z_1 \approx 2.12 \text{ Ohm}^{-1} \text{ m}^{-1}$.

a. *Transmission in the dispersive regime*

Here we consider an effect of the qubit on the transmission coefficient, substituting the qubit by an additional classical inductance coupled to the resonator. This classical analogy may be helpful to understand the quantum-mechanical effect. In the dispersive regime, coupling to the qubit can be described as an additional classical inductance L_{qb} at the position $x = 0$. Such a problem is described by adding two more equations for $x = 0$ to the system of equations (A33-A36), which follows from Eq. (A1) by adding to the r.h.s. the following term

$$-\delta(x)M\frac{\partial I_{\text{qb}}}{\partial t} = -\delta(x)L_{\text{qb}}\frac{\partial I(x,t)}{\partial t}, \quad (\text{A46})$$

where

$$L_{\text{qb}} = M^2\frac{\partial I_{\text{qb}}}{\partial \Phi}. \quad (\text{A47})$$

In the ground state we have [43, 44]

$$L_{\text{qb}} = \frac{4M^2I_p^2\Delta^2}{(\Delta^2 + \varepsilon^2)^{3/2}}. \quad (\text{A48})$$

We modify the definition of V_2 given in Eq. (A31)

$$V_{2l}(x) = V_{2l}^r e^{-\gamma x} + V_{2l}^l e^{\gamma x}, \quad -\frac{l}{2} < x < 0, \quad (\text{A49})$$

$$V_{2r}(x) = V_{2r}^r e^{-\gamma x} + V_{2r}^l e^{\gamma x}, \quad 0 < x < \frac{l}{2}, \quad (\text{A50})$$

then the boundary conditions at $x = 0$ are

$$I_{2l}(0) = I_{2r}(0), \quad (\text{A51})$$

$$V_{2l}(0) = V_{2r}(0) + i\omega L_{\text{qb}}I_{2r}(0). \quad (\text{A52})$$

The solution of the system of equations for the transmission coefficient can be written as

$$t' = \left[\frac{1}{t} - i\frac{\omega L_{\text{qb}}}{8\theta_1^2 Z_0} (e^{-\gamma l} - 1 - i2\theta_1)^2 \right]^{-1} \approx \left[\frac{\varkappa}{\varkappa_{\text{ext}}} \left(1 - i\frac{2}{\varkappa} \left(\delta\omega + \frac{\omega L_{\text{qb}}\varkappa_{\text{ext}}}{4\theta_1^2 Z_0} \right) \right) \right]^{-1} \quad (\text{A53})$$

where t is the transmission without the qubit ($L_{\text{q}} = 0$) from Eq. (A39). Here we used the following simplifications $-\gamma l = -ikl - \alpha l = -i\pi - \alpha l$ and $\alpha l \ll 1$, $\theta_1 \ll 1$. Finally we rewrite t' in the compact form

$$t' \approx \frac{\frac{\varkappa_{\text{ext}}}{\varkappa}}{1 - i\frac{2\delta\omega'}{\varkappa}}, \quad (\text{A54})$$

where detuning $\delta\omega' = \omega_r' - \omega_d$ from the redefined resonance frequency

$$\omega_r' = \omega_r - \frac{\omega_r L_{\text{qb}}\varkappa_{\text{ext}}}{4\theta_1^2 Z_0} = \omega_r \left(1 - \frac{L_{\text{qb}}}{L_r} \right), \quad (\text{A55})$$

which is shifted due to the extra inductance L_{qb} in the resonator. The phase shift of the transmission coefficient t' at $\delta\omega = 0$ is found as

$$\tan \varphi = \frac{\text{Im}[t']}{\text{Re}[t']} = \frac{\omega_r L_{\text{qb}} \varkappa_{\text{ext}}}{2\theta_1^2 Z_0 \varkappa} = \frac{1}{2\pi} \left(\frac{C_r}{C_0} \right)^2 \frac{L_{\text{qb}} \varkappa_{\text{ext}}}{L_r \varkappa}. \quad (\text{A56})$$

In the ground state we obtain

$$\tan \varphi = A \left[1 + (\varepsilon/\Delta)^2 \right]^{-3/2}, \quad (\text{A57})$$

$$A = \frac{2}{\pi} \left(\frac{C_r}{C_0} \right)^2 \frac{\hbar g^2}{\omega_r \Delta}. \quad (\text{A58})$$

b. Resonant transmission

The measured resonator field is expressed via the field operator expectation values $\langle \hat{I} \rangle$ or $\langle \hat{V} \rangle$ (see Eqs. (A24, A25)). Particularly, the expectation value of the voltage at $x = \pm l/2$ is $V_{r0} \langle ia - ia^\dagger \rangle \sin(\pm k_r l/2) \approx \pm V_{r0} \langle ia - ia^\dagger \rangle$, and the positive frequency component of the charge on the capacitances C_0 are

$$\langle q^+ \rangle = \pm C_0 V_{r0} \langle -ia^\dagger \rangle. \quad (\text{A59})$$

The current leaking out from the resonator, expressed via the reflection and transmission coefficients r and t , is a time-derivative of the charge at $x = -l/2$ and $x = l/2$, that is

$$\frac{V_1^r}{Z_1}(1 - r) = i\omega \langle q^+ \rangle. \quad (\text{A60})$$

$$\frac{V_1^r}{Z_1}t = i\omega \langle q^+ \rangle. \quad (\text{A61})$$

Then the transmission coefficient can be presented as

$$t = \frac{i\theta V_{r0} \langle -ia^\dagger \rangle}{V_1^r}, \quad (\text{A62})$$

which after some algebra using Eq. (29) and Eq. (A44) can be rewritten in a simple physical form

$$t = -\frac{\mathcal{Z}_{\text{ext}}}{2(\xi/\hbar)} \langle a^\dagger \rangle. \quad (\text{A63})$$

It is also straightforward to demonstrate that the scattered waves: back scattered $V_1^r e^{ik(x+l/2)}$ at $x < -l/2$ and forward $V_1^r t e^{-ik(x-l/2)} - V_1^r e^{-ik(x-l/2)}$ (difference between the transmitted and the undisturbed one as, if there is no resonator) at $x > l/2$ are equal in amplitude ($1 - r = t$) and, therefore, effectively result in zero interaction energy

$$C_0 V_1^r V_{r0} \sin(k_r l/2) [-r + (1 - t)e^{-ik_r l}] = 0, \quad (\text{A64})$$

(compare with Eq. (28)) that is in the quasi-classical approach of scattering, the first order scattering gives an exact solution.

-
- [1] E. Il'ichev, A.Yu. Smirnov, M. Grajcar, A. Izmalkov, D. Born, N. Oukhanski, Th. Wagner, W. Krech, H.-G. Meyer, and A. Zagoskin, *Low Temp. Phys.* **30**, 620 (2004).
 - [2] J.Q. You and F. Nori, *Physics Today* **58**(11), 42 (2005).
 - [3] G. Wendin and V.S. Shumeiko, arXiv:cond-mat/0508729; *Low Temp. Phys.* **33**, 724 (2007).
 - [4] A. Zagoskin and A. Blais, *Phys. Canada* **63**, 215 (2007).
 - [5] Yu.A. Pashkin, T. Yamamoto, O. Astafiev, Y. Nakamura, D.V. Averin, and J.S. Tsai, *Nature* **421**, 823 (2003).
 - [6] A. Izmalkov, M. Grajcar, E. Il'ichev, Th. Wagner, H.-G. Meyer, A.Yu. Smirnov, M.H.S. Amin, Alec Maassen van den Brink, and A.M. Zagoskin, *Phys. Rev. Lett.* **93**, 037003 (2004).
 - [7] D. Vion, A. Aassime, A. Cottet, P. Joyez, H. Pothier, C. Urbina, D. Esteve, and M. H. Devoret, *Science* **296**, 886 (2002).
 - [8] I. Chiorescu, Y. Nakamura, C. J. P. M. Harmans, and J. E. Mooij, *Science* **299**, 1869 (2003).
 - [9] I. Chiorescu, P. Bertet, K. Semba, Y. Nakamura, C. J. P. M. Harmans, and J. E. Mooij, *Nature* **431**, 160 (2004).
 - [10] E. Il'ichev, N. Oukhanski, A. Izmalkov, Th. Wagner, M. Grajcar, H.-G. Meyer, A.Yu. Smirnov, Alec Maassen van den Brink, M.H.S. Amin, and A.M. Zagoskin, *Phys. Rev. Lett.* **91**, 097906, (2003).
 - [11] J. Johansson, S. Saito, T. Meno, H. Nakano, M. Ueda, K. Semba, and H. Takayanagi, *Phys. Rev. Lett.* **96**, 127006 (2006).
 - [12] A.N. Omelyanchouk, S. Savel'ev, A. M. Zagoskin, E. Il'ichev, and F. Nori, *Phys. Rev B* **80**, 212503 (2009).
 - [13] Y. Nakamura, Yu.A. Pashkin, T. Yamamoto, and J. S. Tsai, *Phys. Rev. Lett.* **88**, 047901 (2002).
 - [14] D. Vion, A. Aassime, A. Cottet, P. Joyez, H. Pothier, C. Urbina, D. Esteve, and M.H. Devoret, *Fortschr. Phys.* **51**, 462 (2003).
 - [15] A. Izmalkov, M. Grajcar, E. Il'ichev, N. Oukhanski, Th. Wagner, H.-G. Meyer, W. Krech, M.H.S. Amin, Alec Maassen van den Brink, and A.M. Zagoskin, *Europhys. Lett.* **65**, 844 (2004).
 - [16] W.D. Oliver, Ya. Yu, J.C. Lee, K.K. Berggren, L.S. Levitov, and T.P. Orlando, *Science* **310**, 1653 (2005).
 - [17] M. Sillanpää, T. Lehtinen, A. Paila, Yu. Makhlin, and P. Hakonen, *Phys. Rev. Lett.* **96**, 187002 (2006).
 - [18] S.N. Shevchenko, S. Ashhab, and F. Nori, *Phys. Rep.* **492**, 1 (2010).
 - [19] G. Sun, X. Wen, B. Mao, J. Chen, Y. Yu, P. Wu, and S. Han, *Nat. Commun.* **1**, 51 (2010).
 - [20] R. J. Schoelkopf and S. M. Girvin, *Nature* **451**, 664 (2008).

- [21] A. Blais, R.-S. Huang, A. Wallraff, S.M. Girvin, and R.J. Schoelkopf, *Phys. Rev. A* **69**, 062320 (2004).
- [22] Y.X. Liu, C.P. Sun, and F. Nori, *Phys. Rev. A* **74**, 052321 (2006).
- [23] Y.-L. Chen, Y.-F. Xiao, X. Zhou, Xu-Bo Zou, Z.-W. Zhou and G.-C. Guo, *J. Phys. B: At. Mol. Opt. Phys.* **41**, 175503 (2008).
- [24] J. Bourassa, J. M. Gambetta, A. A. Abdumalikov Jr., O. Astafiev, Y. Nakamura, and A. Blais, *Phys. Rev. A* **80**, 032109 (2009).
- [25] S. Ashhab and F. Nori, *Phys. Rev. A* **81**, 042311 (2010).
- [26] A. Wallraff, D. I. Schuster, A. Blais, L. Frunzio, R.-S. Huang, J. Majer, S. Kumar, S. M. Girvin, and R. J. Schoelkopf, *Nature* **431**, 162 (2004).
- [27] D. I. Schuster, A. Wallraff, A. Blais, L. Frunzio, R.-S. Huang, J. Majer, S.M. Girvin, and R. J. Schoelkopf, *Phys. Rev. Lett.* **94**, 123602 (2005).
- [28] D. I. Schuster, *Circuit Quantum Electrodynamics*, PhD thesis, Yale University, 2007.
- [29] T. Lindström, C.H. Webster, J.E. Healey, M.S. Colclough, C.M. Muirhead, and A.Y. Tzalenchuk, *Supercond. Sci. Technol.* **20**, 814 (2007).
- [30] A.A. Abdumalikov, Jr., O. Astafiev, Y. Nakamura, Yu.A. Pashkin, and J.S. Tsai, *Phys. Rev. B* **78**, 180502(R) (2008).
- [31] G. Oelsner, S.H.W. van der Ploeg, P. Macha, U. Hübner, D. Born, S. Anders, E. Il'ichev, H.-G. Meyer, M. Grajcar, S. Wünsch, M. Siegel, A.N. Omelyanchouk, and O. Astafiev, *Phys. Rev. B* **81**, 172505 (2010).
- [32] T.P. Orlando, J.E. Mooij, L. Tian, C.H. van der Wal, L.S. Levitov, S. Lloyd, and J.J. Mazo, *Phys. Rev. B* **60**, 15399 (1999).
- [33] O. Astafiev, A.M. Zagoskin, A.A. Abdumalikov Jr., Yu.A. Pashkin, T. Yamamoto, K. Inomata, Y. Nakamura, and J.S. Tsai, *Science* **327**, 840 (2010).
- [34] L. Zhou, Z.R. Gong, Y.X. Liu, C.P. Sun, and F. Nori, *Phys. Rev. Lett.* **101**, 100501 (2008).
- [35] S.N. Shevchenko, S.H.W. van der Ploeg, M. Grajcar, E. Il'ichev, A.N. Omelyanchouk, and H.-G. Meyer, *Phys. Rev. B* **78**, 174527 (2008).
- [36] Ya.S. Greenberg, *Phys. Rev. B* **76**, 104520 (2007).
- [37] J.M Fink, M. Göppl, M. Baur, R. Bianchetti, P.J. Leek, A. Blais, and A. Wallraff, *Nature* **454**, 315 (2008).
- [38] W.P. Schleich, *Quantum Optics in Phase Space* (Wiley-VCH, Berlin) (2001).
- [39] M.O. Scully and M.S. Zubairy, *Quantum Optics* (Cambridge, Cambridge University Press) (1997).
- [40] L.S. Bishop, J.M. Chow, J. Koch, A.A. Houck, M.H. Devoret, E. Thuneberg, S.M. Girvin, and R. J. Schoelkopf, *Nature Phys.* **5**, 105 (2009).
- [41] D.M. Pozar, *Microwave Engineering* (Wiley, New York, 3rd ed.) (1990).
- [42] P. Macha, S.H.W. van der Ploeg, G. Oelsner, E. Il'ichev, H.-G. Meyer, S. Wünsch, and M. Siegel, *Appl. Phys. Lett.* **96**, 062503 (2010).
- [43] Ya.S. Greenberg, A. Izmalkov, M. Grajcar, E. Il'ichev, W. Krech, H.-G. Meyer, M. H. S. Amin, and A. Maassen van den Brink, *Phys. Rev. B* **66**, 214525 (2002).
- [44] M. Grajcar, A. Izmalkov, E. Il'ichev, Th. Wagner, N. Oukhanski, U. Hübner, T. May, I. Zhilyaev, H. E. Hoenig, Ya. S. Greenberg, V. I. Shnyrkov, D. Born, W. Krech, H.-G. Meyer, Alec Maassen van den Brink, and M. H. S. Amin, *Phys. Rev. B* **69**, 060501(R) (2004).